THE ASTROPHYSICAL JOURNAL, 296:481–491, 1985 September 15

MOLECULAR CLOUDS IN M31 AND M33

LEO BLITZ[1]
University of Maryland
Received 1984 December 6; accepted 1985 March 11

ABSTRACT

In order to determine the properties of the molecular clouds in nearby spiral galaxies, 49 H II regions in M31 and 6 H II regions in M33 were observed using the $J = 1 \rightarrow 0$ transition of CO. Of these, 17 were detected in M31 and two in M33. For the CO detection in M31, $\langle T_R^* \rangle = 0.14$ K, $\langle \Delta V \rangle = 12.5$ km s^{-1}, and $\langle T_R^* \Delta V \rangle = 2.1$ K km s^{-1}. The two detections in M33, which are toward the giant H II regions NGC 604 and NGC 595, are somewhat weaker than the mean values for clouds in M31. In M31, neither T_R^* nor ΔV shows any gradient with galactic radius, but $\langle T_R^* \Delta V \rangle$ is a decreasing function of radius. The mean values of $\langle \Delta V \rangle$ and $\langle T_R^* \Delta V \rangle$ are considerably larger than the values that would be obtained by extrapolating local giant molecular clouds to the distance of M31. It is suggested that most of the CO emission is from small clouds in the beam which overwhelm the emission from the giant molecular clouds. Some observational tests of this suggestion are proposed. Like the molecular clouds in the Milky Way, the giant molecular clouds in M31 appear to be tidally limited. In M33 the larger inclination angle would make the observed contribution from small molecular clouds less significant, which is consistent with the observations. In spite of the virulent star formation in NGC 604 and NGC 595, the molecular emission with which they are associated is unremarkable.

Subject headings: galaxies: individual — interstellar: molecules — nebulae: H II regions — nebulae: individual

I. INTRODUCTION

A large fraction of the giant molecular cloud complexes (GMCs) in the vicinity of the Sun have been observed in sufficient detail to determine their large-scale properties (Blitz 1978, 1980; Wouterloot 1981, 1984*a*, *b*). Surveys of the inner Galaxy (Stark 1983; Sanders, Solomon, and Scoville 1984; Dame 1983), and maps of some giant clouds at galactocentric distances as large as 15 kpc (Kutner and Mead 1981) have allowed these properties to be extrapolated to other regions of the Milky Way. These studies and many others have shown conclusively that the giant molecular cloud complexes are the sites of most, if not all, present-day Galactic star formation. But how do the sites of star formation in the Milky Way compare with those in other spiral galaxies?

For example, the molecular gas content of M31 is known to be significantly lower than that of the Milky Way (Stark 1985). Does that imply that the properties of the GMCs in M31 are different from those in the Milky Way? Stark and Blitz (1978) have argued that the size of a GMC in the Milky Way is limited by Galactic tidal forces. Is the same true for M31? There are no H II regions in the Milky Way as spectacular as NGC 604 or NGC 595 in M33 (Israel and van der Kruit 1974). Do these extraordinary H II regions form from extraordinary molecular clouds?

In order to attempt to answer these questions, 49 GMCs in M31 and six GMCs in M33 were observed using the $J = 1 \rightarrow 0$ transition of CO. In the Milky Way, 75%–80% of all H II regions have associated molecular clouds (Blitz, Fich, and Stark 1982); the percentage is likely to be higher for the brightest H II regions. H II regions were thus used as indicators of the locations of their parent GMCs. M31 and M33 were chosen because they are the most distant spiral galaxies for which individual GMCs could be studied with the instruments available when the first observations were made. New large millimeter telescopes and interferometers will ultimately be able to extend these observations beyond the Local Group.

II. OBSERVATIONS

The sources chosen for observation were taken from the H II region catalog of Baade and Arp (1964) in the case of M31, and from that of Israel and van der Kruit (1974) in the case of M33. In M31, H II regions were observed over a range of galactocentric distance R from 3 to 19 kpc. To minimize the likelihood of getting more than one GMC in the beam at a time, observations were generally made in directions where only a single H II region would fall in the beam (except as noted in Table 1). No selection was made on the basis of brightness, but the Baade and Arp catalog selects objects of relatively high surface brightness. In M33, the H II regions observed were those with the highest 6 cm radio fluxes, as measured by Israel and van der Kruit (1974).

The CO $J = 1 \rightarrow 0$ observations were made over a period from 1979 to 1983 at the 11 m NRAO[2] telescope at Kitt Peak. All observations were made with the cooled dual-channel receiver, which produced typical single-sideband noise temperatures of 450 K. Observations were made with the 1 MHz filter banks, which provide a velocity resolution of 2.6 km s^{-1} at the CO frequency. All observations were made in the position-switching mode. On occasion, pairs of H II regions well separated in velocity were observed by placing one in the signal and the other in the reference beam. Sources were generally observed for a total on-source integration time of 1 hour, which produced typical rms noise temperatures of 40 mK.

III. RESULTS

Tables 1 and 2 summarize the results of the observations of M31 and M33, respectively. For M31, the H I velocities are

[1] Alfred P. Sloan Foundation Fellow.

[2] The National Radio Astronomy Observatory is operated under contract by Associated Universities, Inc., for the National Science Foundation.

TABLE 1

CO OBSERVATIONS OF M31

A. DETECTIONS

Source (BA)	R (kpc)	V(H I)[a] (km s^{-1})	V(CO) (km s^{-1})	T_R^* (mK)	ΔV (km s^{-1})
108[b]	8.8	−204	−190 ± 2	260 ± 70	21.8 ± 4.2
143[c]	9.2	−182	−154 ± 2	130 ± 60	17.2 ± 6.2
149	5.9	−55	−55 ± 1	110 ± 20	22.4 ± 3.9
163[d]	9.4	−125	−126 ± 1	210 ± 50	13.5 ± 3.1
210[e]	10.5	−65	−55 ± 1	210 ± 70	13.0 ± 3.9
248	17.3	−80[f]	(−90 ± 2)	(100 ± 40)	(10.4 ± 4.2)
253	7.5	−335	−339 ± 1	190 ± 40	14.6 ± 2.3
284	9.1	−407	−398 ± 1	130 ± 50	10.9 ± 3.1
286[e]	9.1	−420	−400 ± 1	210 ± 50	13.0 ± 2.6
297	9.8	−450	−433 ± 1	140 ± 60	21.3 ± 6.5
305	10.3	−495	(−487 ± 3)	(150 ± 70)	(7.8 ± 2.6)
312	8.7	−576	−567 ± 1	100 ± 20	15.6 ± 2.3
320	10.6	−525	−529 ± 1	150 ± 20	14.0 ± 1.8
423	4.7	−457	−463 ± 1	150 ± 50	18.2 ± 2.3
450	8.1	−584	−480 ± 1	110 ± 40	6.2 ± 2.3
460	8.2	−524	−533 ± 1	90 ± 30	12.0 ± 2.6
		−562	...	...	...
484[e]	12.9	−555	(−531 ± 2)	(100 ± 40)	15.6 ± 5.7
514	7.5	−300	−311 ± 3	130 ± 50	6.5 ± 2.6
			−297 ± 1	210 ± 80	11.4 ± 3.6
612[e]	9.7	−70	−59 ± 1	310 ± 40	10.4 ± 2.6
626	9.7	−65	−58 ± 1	230 ± 70	7.0 ± 2.6

B. NONDETECTIONS

Source (BA)	R (kpc)	V(H I) (km s^{-1})	T_{rms} (mK)	Comments
55	3.2	(−244)	60	H I velocity uncertain; T_{rms} = 0.01 at 7 m (Bell Laboratories)[g]
196	9.3	−64	100	possible line at V = −33.6
242	13.9	−44	40	
251	8.0	−321	60	
259	7.9	−354	60	
269[e]	6.1	−399	90	possible line at V = −405
277	9.9	−376	...	possible line at V = −349; spectrum poor due to bad baseline
290	9.4	−419	40	
330	12.1	−474	40	
334	10.8	−555	60	
343	12.0	−535	40	
352	14.0	−536	50	
360[d]	13.9	−530	60	
379	13.5	−545	50	
401	10.6	−344	70	
412	10.6	−354	40	
415	3.5	(−390)	40	H I velocity uncertain
416	4.5	−442	50	
452	11.7	−374	100	
		−411		possible line at V = −380
464	8.3	−560	50	
465	9.0	−530	50	
500[h]	19.3	−570	100	velocity from Rubin and D'Odorico 1969
513	9.4	−275	70	
565	11.0	−205	50	
581	11.6	−161	50	
628	14.6	−114	60	
665[i]	14.0	−54	90	
672[i]	14.1	−54	70	
683	17.5	−120	80	velocity from Rubin and D'Odorico 1969

[a] From Brinks 1984.
[b] Six H II regions in beam.
[c] Seven H II regions in beam.
[d] Four H II regions in beam.
[e] Two H II regions in beam.
[f] Velocity from Rubin and D'Odorico 1969.
[g] Stark 1984, unpublished observation.
[h] Three H II regions in beam.
[i] Ten H II regions in beam.

TABLE 2

CO OBSERVATIONS OF M33

Source	R (kpc)	V(H I)[a] (km s^{-1})	V(CO) (km s^{-1})	T_R^*(CO) (mK)	ΔV (km s^{-1})	M(H II)[b] ($M_\odot$)
NGC 595 ...	1.7	−183	−185.7	130	7.6	4.9×10^5
NGC 604 ...	3.0	−236	−244.7	100	13.3	2.2×10^6
IK 25.....	1.2	−135	(−135.7)	(120)	(11.7)	3.5×10^4
IK 50.....	0.6	−203	(−187.7)	(180)	(9)	4.5×10^4
IK 49.....	1.5	−146	...	<40	...	4.4×10^4
IK 18.....	2.0	−206	...	<60	...	8.4×10^4

[a] From Rogstad, Wright, and Lockhart 1976.
[b] From Israel and van der Kruit 1974.

from Brinks (1984). In a few cases where these are not available, velocities are taken from Rubin and D'Odorico (1969). For M33, the H I velocities are from Rogstad, Wright, and Lockhart (1976), and the masses of the H II regions are from Israel and van der Kruit (1974). The quantities V(H I) and V(CO) are given with respect to the local standard of rest, and ΔV is the full width at half-maximum. The line parameters are determined from Gaussian fits to the lines, and the uncertainties in V_{CO}, T_R^*, and ΔV are the 1 σ uncertainties of the Gaussian fits. Representative spectra are shown in Figure 1.

The results from the 11 m telescope are reported in units of T_R^* following Kutner and Ulich (1981). Observations made at other telescopes, generally reported as T_A^*, are compared with these results in § IV, but no attempt has been made to reconcile the temperature scales. Differences should generally be less than ~25% and do not alter any of the conclusions.

IV. DISCUSSION

a) M31

A histogram of the distribution of the number of objects observed and the number and percentage of objects detected in M31 as a function of galactic radius is given in Figure 2. The figure shows a concentration toward $R = 9$ kpc, which reflects the larger galactocentric radius of the peak of the molecular annulus in M31 by comparison with the Milky Way. The figure also implies that it is reasonable to compare the mean properties of the GMCs detected in M31 with those in the solar vicinity. The detection percentage counts a possible detection as half of a definite detection. No clouds were definitely detected at distances greater than 12 kpc from the center of M31.

i) *Comparison with Local GMCs*

A review of the properties of local GMCs has been given by Blitz (1980). He finds that the mean projected surface area of 12 GMCs is 2.1×10^3 pc^2 when observed to a sensitivity of 1 K at a resolution of 2.6 km s^{-1}. From an extrapolation of the boundaries of three local GMCs, Blitz and Thaddeus (1980) find that if the observations were made using a telescope with infinite sensitivity, the measured surface area would increase by less than 50%. A similar analysis was performed by Wouterloot (1981) using OH observations, which confirmed the results of Blitz and Thaddeus (1980). The expected contribution to the CO luminosity of gas below the 2.6 K km s^{-1} sensitivity limit is ~20%. The mean surface area of 2.1×10^3 pc^2 of a local GMC will therefore be assumed to contain 80% of the CO luminosity and thus 80% of the H_2 mass.

From maps of three local GMCs, Blitz (1978, 1980) finds the mean velocity-integrated antenna temperature, I(CO), to be 8.8 K km s^{-1} measured with the Columbia Sky Survey Telescope. This value is an average over all positions at which CO was detected above the sensitivity limit. The corresponding mean peak $\langle T_A^* \rangle$ is 1.9 K, and the mean line width ΔV is 4.7 km s^{-1}. The mean peak T_A^* and I(CO) must be scaled up by 35% as a result of a recalibration of the Columbia dish (Dame 1983). The mean observed values for local GMCs are therefore as follows:

$$T_A^* = 2.6 \text{ K} ,$$

$$\sum T_A^* \Delta V = 11.9 \text{ K km s}^{-1} ,$$

$$\Delta V = 4.7 \text{ km s}^{-1} ,$$

$$\text{projected area} = 2.1 \times 10^3 \text{ pc}^2 .$$

These are the mean values that would be observed for local GMCs using a telescope with a beam efficiency of ~0.7 observed at a resolution of 2.6 km s^{-1} (1 MHz) and averaged over the entire cloud. Galactic molecular clouds observed with a velocity resolution <2.6 km s^{-1} generally give line parameters different from the above values. Typical CO line widths (FWHM) are 2–3 km s^{-1}; thus, when observations are made with a velocity resolution less than 1 km s^{-1}, T_A^* for a typical line of sight is ~4–6 K. Nevertheless, the values quoted above are the best values to compare with extragalactic CO $J = 1$–0 observations, since these are usually made with 1 MHz frequency resolution.

The value for ΔV above reflects the random motion of clumps within a GMC and is therefore a measure of its total kinetic energy. The corresponding one-dimensional velocity dispersion for the CO within a GMC is 2.0 km s^{-1}. For a spherical homogeneous cloud with a projected surface area of 2.1×10^3 pc, this corresponds to a mass of 1.2×10^5 $M_\odot$ for a cloud in virial equilibrium. This value is in good agreement with the masses of (1–2) $\times 10^5$ $M_\odot$ derived for most GMCs in the solar neighborhood, based on an LTE analysis of the CO line strengths (Blitz 1980), and from considerations of their stability against the Galactic tidal field (Stark and Blitz 1978).

ii) *Extrapolation to M31*

M31 is at a distance of ~700 kpc. At this distance, the 66″ beam of the 11 m telescope subtends 200 pc. The beam filling fraction for a local GMC would therefore be 5.5×10^{-2}. Table 3 presents the observational parameters one would expect for a local GMC at the distance of M31 (or M33) observed at a resolution of 2.6 km s^{-1} and assuming a beam efficiency of 0.7. These are compared with the weighted mean values observed for the CO clouds in M31 (the unweighted mean values are somewhat higher). The fourth column gives the dispersion of the observed values. The mean peak antenna temperature of the detected clouds corresponds closely to the extrapolated local value, but the observed line widths and the velocity-integrated antenna temperatures are much larger than expected. Let us examine several possibilities for the differences from extrapolated local GMC values.

TABLE 3

CO IN GMCs IN M31

Quantity	Expected	Observed	Dispersion
$\langle T_A^* \rangle$ (K)	0.14	0.14 ± 0.01	0.06
$\langle T_A^* \Delta V \rangle$ (K km s^{-1})	0.66	2.1 ± 0.1	1.1
$\langle \Delta V \rangle$ (km s^{-1})	4.7	12.5 ± 0.6	4.8

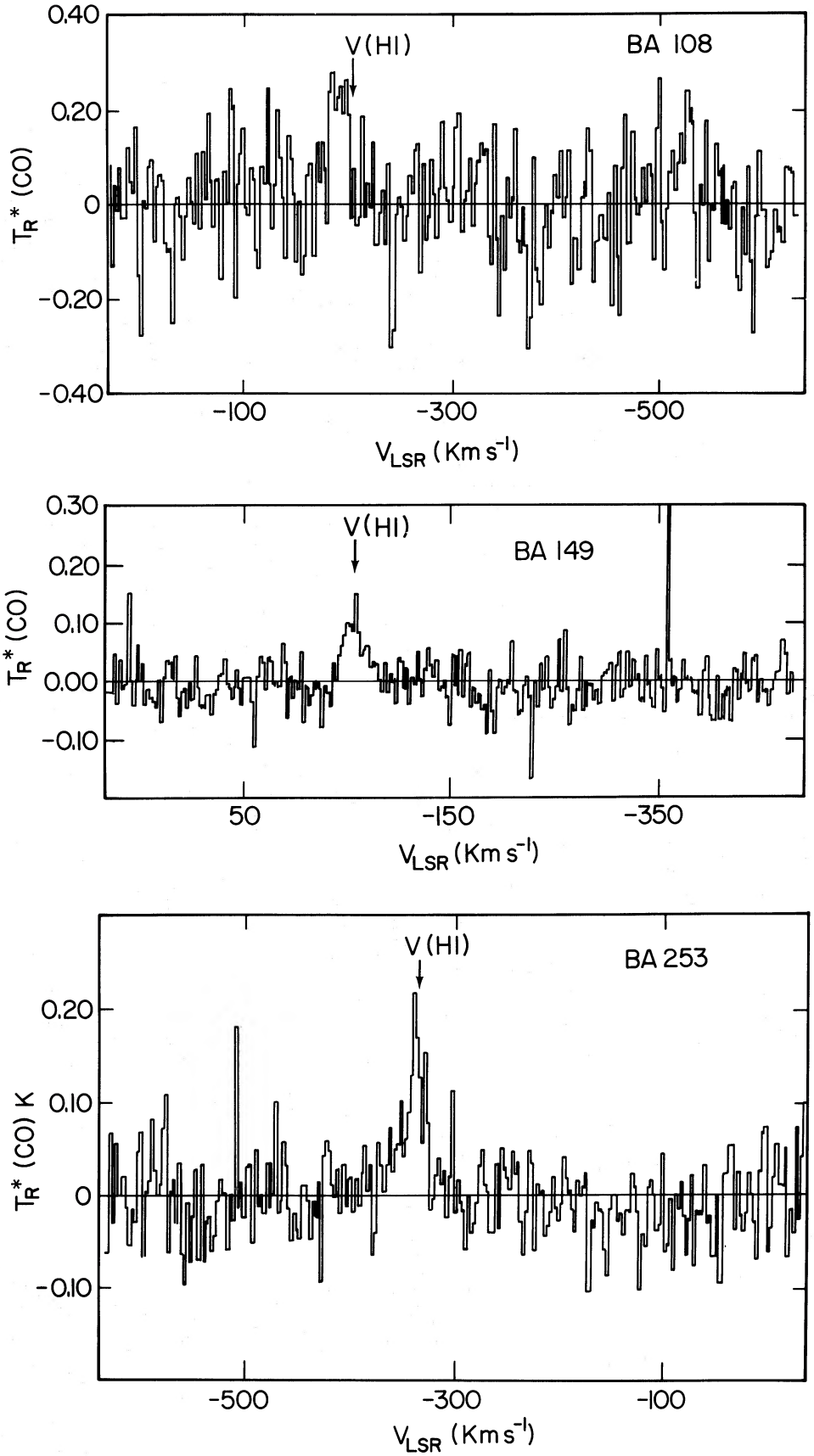

FIG. 1.—CO spectra toward five of the H II regions detected in M31 and the two detected in M33. In each case, the H I velocity is indicated.

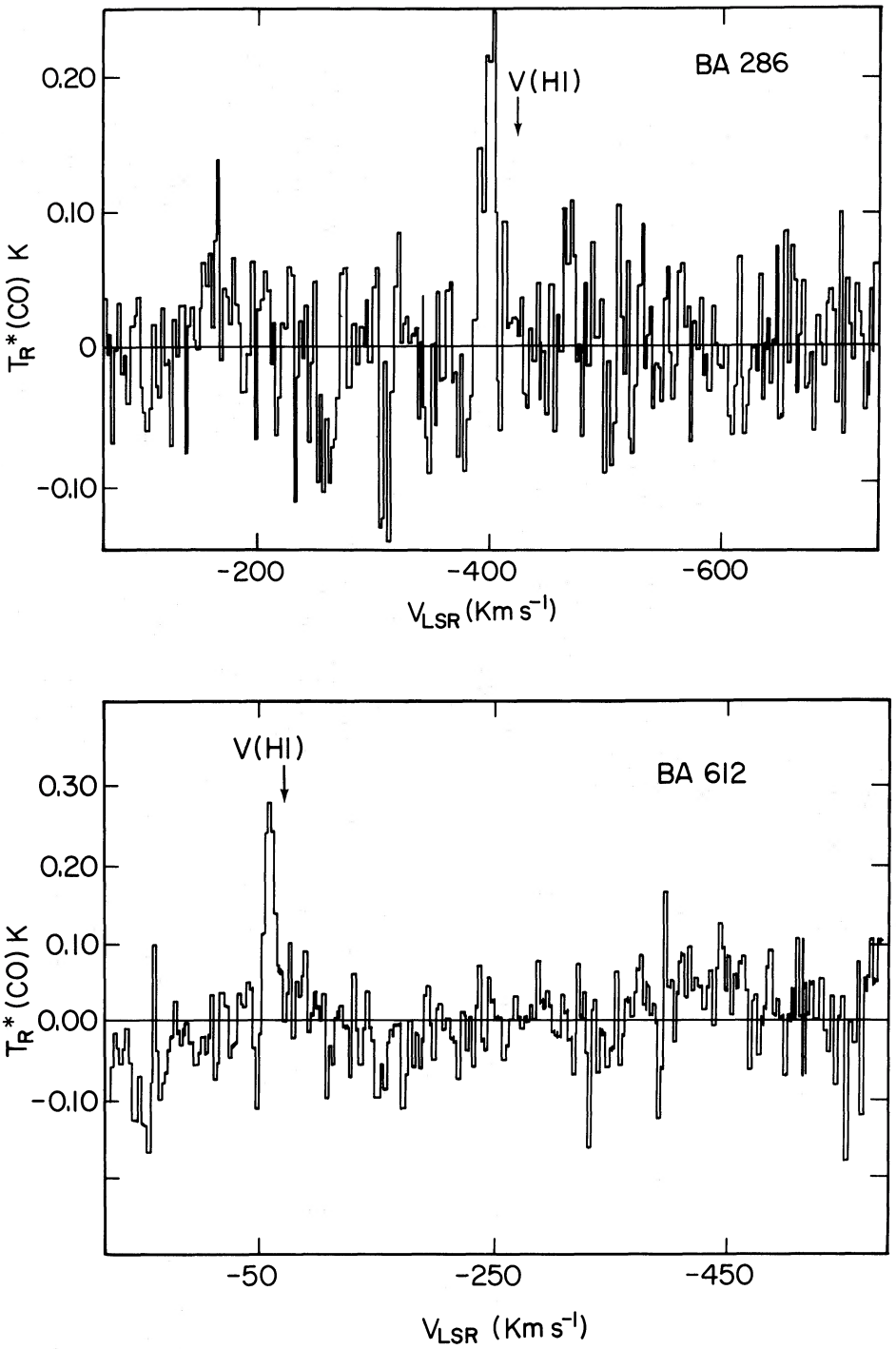

FIG. 1.—*Continued*

1. *GMCs in virial equilibrium.*—If all of the emission is from a single GMC in each case (which is probably not the case for at least some of the H II regions in Table 1), and if the clouds are in virial equilibrium, the large line widths imply that the clouds are an order of magnitude more massive than their counterparts in the solar vicinity. The total CO emission from each complex is, however, only a factor of 3 greater than that of Galactic GMCs. If the M31 clouds are both smaller (by about a factor of 3 in projected surface area) and about 3 times more massive than Galactic GMCs, the expected and observed values can be made to agree. In this case, the increased mass and increased size would offset any change in the expected $\langle T_A^* \rangle$, but each factor of 3 would contribute a $\sqrt{3}$ increase in the velocity dispersion and consequently in $\langle T_A^* \Delta V \rangle$. This explanation for the observed difference of the M31 and local GMCs has the disadvantage of being entirely ad hoc. Further-

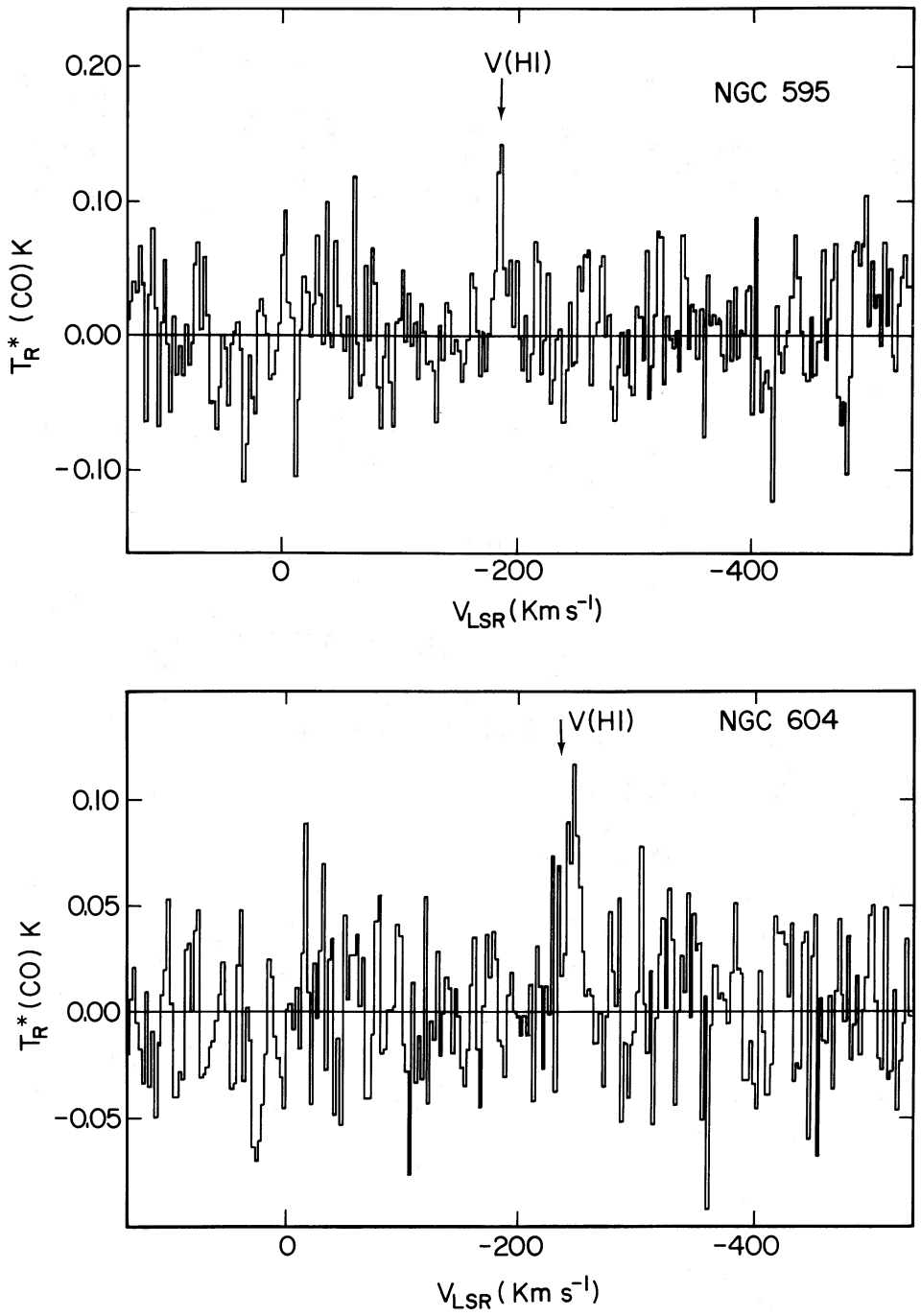

FIG. 1.—*Continued*

more, unlike their Galactic counterparts, the small, massive clouds in M31 would be completely out of equilibrium with its tidal field (see § IV*a*[iii]). Let us consider other sources for the differences in Table 3.

2. *Rotation of the complexes.*—A number of local GMCs exhibit large-scale velocity gradients which have been interpreted as rotation (e.g., Kutner *et al.* 1977; Lada *et al.* 1978; Blitz and Thaddeus 1980). In a few instances, the velocity gradients are quite large and could, in principle, broaden the lines seen in M31. The velocity-integrated line temperature, $\sum T_A^* \Delta V$, is, however, a conserved quantity for an unresolved cloud, irrespective of any large-scale gradients. Thus, if rotation of the complexes increased the expected ΔV in Table 3, then the expected value of $\langle T_A^* \rangle$ would decrease by the same factor. Furthermore, to obtain a value for ΔV of 15 km s^{-1}, the *mean* velocity gradients in M31 would have to be comparable to the largest gradients observed for local GMCs. Although rotation may broaden the CO lines somewhat, it cannot be

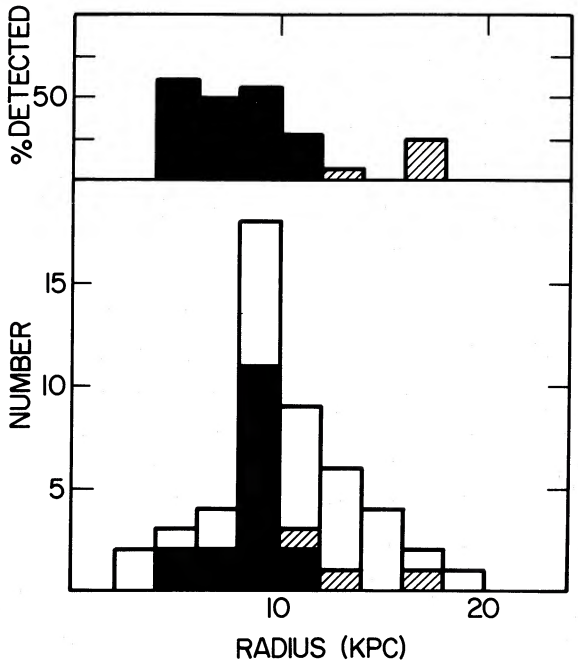

FIG. 2.—Histogram of the number of detections (*dark bars*), probable detections (*shaded bars*) and nondetections (*unshaded bars*) as a function of galactic radius, binned in 2 kpc radial bins. The upper portion of the figure shows the detection percentage as a function of radius; the probable detections are counted as half. Beyond 12 kpc, the CO associated with the H II regions tends to be below the detection limit of ~ 1 K km s^{-1}.

responsible for the differences found in the expected and observed line parameters in M31.

3. *Small molecular clouds.*—Recently, large numbers of small molecular clouds have been discovered in the solar vicinity (Blitz, Magnani, and Mundy 1984). These may be pervasive in the Galaxy, or at least in the spiral arms. Indeed, Boulanger, Stark, and Combes (1981) have argued that the wide CO profiles they observed in a spiral arm segment of M31 suggest the presence of a number of small molecular clouds in the beam. The intrinsic cloud-to-cloud velocity dispersion of such clouds and velocity gradients in the beam due to differential galactic rotation could be responsible for the large line widths seen in M31.

Blitz, Magnani, and Mundy (1984) find a velocity dispersion of 5.7 km s^{-1} for the local high-latitude molecular clouds. An ensemble of such clouds observed from outside the Milky Way would produce a line width of 13.4 km s^{-1}, in good agreement with the observed lines in M31. Is $\langle T_A^* \Delta V \rangle$ consistent with the locally observed surface density of small molecular clouds? The mean $\langle T_A^* \Delta V \rangle$ of the local clouds is 2.6 K km s^{-1}, and the surface filling fraction viewed from the Sun is $2.5 \times 10^{-3}/\epsilon$, where ϵ is the completeness of the high-latitude survey. The value of ϵ is now known to be <0.83 (Magnani, Blitz, and Mundy 1985); assuming a value of 0.5 for ϵ, the surface filling fraction of small clouds viewed from outside the Galaxy would be 1×10^{-2} if observed normal to the plane. If observed at the inclination of M31 (taken to be 77°), the surface filling fraction is $\sim 5 \times 10^{-2}$, the expected $\langle T_A^* \rangle$ is ~ 0.13 K, and $\langle T_A^* \Delta V \rangle$ is ~ 1.7 K km s^{-1}, values remarkably close to the observed ones. Thus, the best current estimate for the properties and numbers of small local molecular clouds indicates that they could be responsible for most of the CO emission seen toward H II regions in M31.

4. *Differential rotation within the beam.*—Differential rotation of M31 within the 1.1 NRAO beam does not alter this conclusion, although its effects are nonnegligible. The effects of differential rotation have been discussed previously by Boulanger, Stark, and Combes (1981). Following their analysis for an ensemble of small clouds, we write

$$\Delta V_{\rm CO}^2 = \Delta V_c^2 + \Delta V_t^2 + \Delta V_B^2 ,$$

where $\Delta V_{\rm CO}$ is the observed CO line width, ΔV_c is the contribution to the line width from cloud-to-cloud velocity dispersions, ΔV_t is the broadening due to the thickness of the CO clouds in the galactic plane and ΔV_B is due to velocity gradients in the plane due to differential rotation.

To estimate ΔV_B, the velocity gradient across the projected beam was measured from a theoretical isovelocity contour map kindly provided by A. A. Stark, prepared from the rotation curve of Rubin and D'Odorico (1969). ΔV_t is equal to $(\partial v/\partial y)h \cos i$, where $\partial v/\partial y$ is the velocity gradient parallel to the minor axis, h is the full scale height of the CO (taken to be 100 pc), and i is the inclination angle. The value of $\langle \Delta V_B \rangle$ is 8.9 km s^{-1}, and $\langle \Delta V_t^2 \rangle$ is 5.4 km s^{-1}. Thus, if $\langle \Delta V_c \rangle$ is equal to the local value of 13.4 km s^{-1}, the increase in the CO line widths compared with the contribution from ΔV_c alone is relatively small, but not completely negligible. The mean total expected CO velocity width is 17.0 km s^{-1}, somewhat larger than the observed value of 14.5 km s^{-1}. It therefore appears that small molecular clouds in the beam similar to those found in the solar vicinity are capable of producing the observed CO line strengths and widths in M31. The observed line widths are, however, somewhat smaller than the predicted values when account is taken of differential rotation within the beam. This explanation implies that the properties of the small CO clouds (mean antenna temperature, surface filling fraction) together with the large inclination angle of M31 coincidentally produce an expected $\langle T_A^* \rangle$ just equal to that expected for GMCs.

It appears that there are three interpretations consistent with the observed data: (1) the CO emission associated with H II regions in M31 is due almost entirely to GMCs which are both smaller and more massive than the ones observed locally; (2) the CO emission is due almost entirely to many small molecular clouds in the beam with observed properties similar to those in the solar vicinity; and (3) the CO emission is due to giant molecular clouds similar to those in the solar vicinity as well as to many small clouds in the beam. Roughly 70% of the emission is from small clouds to account for the observed line parameters.

iii) *Observational Tests*

The present observations alone cannot distinguish between these possibilities, but the explanations are amenable to observational tests. (1) Since the giant molecular clouds would not be resolved by beams $\geq 15''$–$30''$, the observed T_A^* of a cloud should increase as the inverse square of the beam diameter (down to $\sim 15''$, depending on the shape of the cloud and how well it is centered in the beam). The observed line width would be ~ 5–8 km s^{-1}, depending on the degree of rotation of the cloud. (2) If there are many small clouds in the beam, the emission from these clouds will remain constant with decreasing beam size. With increasing beam size, the lines will get broader (depending on the position in the galaxy) as a result of galactic differential rotation, but the peak T_A^* will not increase. Lines of similar strength (but differing width) would be detectable everywhere within a spiral arm (observations at Bell

Laboratories [Linke 1982; Stark 1985] indicated that even small molecular clouds are deficient in the interarm region). (3) If CO emission were from both GMCs *and* small molecular clouds, high-resolution observations ($\leq 30''$) separated by $\sim 1'$ on and off the H II region should both produce detectable lines, but the lines on the source should be stronger by about a factor of 2.

The observations of Boulanger, Stark, and Combes (1981) made with the 1.7 Bell Laboratories beam provide some information as to which is the most likely explanation for the CO emission. They detected CO emission from 11 positions along a spiral arm segment of M31; four of their positions were in the direction of Baade and Arp objects. The following mean values are derived from their observations: $\langle T_A^* \rangle = 0.12$ K, $\langle \Delta V \rangle = 22$ km s^{-1}, $\langle T_A^* \Delta V \rangle = 3.2$ K km s^{-1}. For the directions in which Baade and Arp H II regions are included in the beam, $\langle T_A^* \Delta V \rangle = 3.9$ K km s^{-1}; for the directions in which they are not included, $\langle T_A^* \Delta V \rangle = 2.7$ K km s^{-1}. Thus, the Bell Laboratories detections are wider, but not much weaker, than the Kitt Peak observations. There is emission at levels comparable to that found at NRAO even if there is no cataloged H II region in the beam, but the CO emission is more intense, on average, at positions in which there is an H II region. Comparison of the present observations with those of Boulanger, Stark, and Combes (1981) therefore suggests that the CO emission observed at NRAO is from both GMCs *and* small clouds comparable to those observed locally, but even at a 1.1 resolution the emission is still dominated by the small clouds.

Recently, Boulanger *et al.* (1984) and Ichikawa *et al.* (1985) have made high-resolution CO observations (33″ and 14″ HPBW, respectively) at a number of positions in the southwest arm segment mapped by Linke (1982). Neither set of observations included an H II region; thus these high-resolution observations are not the direct tests suggested above. In both cases, however, there is support for the presence of large massive clouds in addition to diffuse emission from numerous small clouds in the beam. Boulanger *et al.* detect stronger, narrower emission with the 33″ beam than do observations made of the same region with a 1.7 beam. They argue for the existence of a single large cloud complex with a mean diameter of 100–200 pc. If this interpretation is confirmed, the present observations suggest that this complex is unusually large, since emission from it observed with a 1.1 beam would be stronger than emission from any of the 49 objects listed in Table 1 (with the possible exception of BA 108). Ichikawa *et al.* also find evidence for large clouds embedded in diffuse emission from narrow (3–5 km s^{-1}) velocity components superposed on broader emission features.

Blitz and Mathieu (in preparation) have recently made observations at 30″ resolution toward a number of the H II regions presented here using the $J = 2$–1 transition of CO with the 12 m telescope at NRAO. These observations provide a definitive, quantitative test of the predictions made in this section.

iv) *Tidal Stability*

Figure 3 is a histogram of the integrated line strengths of the complexes detected in M31. The decline in number toward low values of $\sum T_R^* \Delta V$ is probably due to the sensitivity limits of these observations, but the sharp cutoff above 3 K km s^{-1} is a real limit. A similar cutoff of 0.3 K is seen for T_R^* in Table 1. Of the 49 clouds observed, only the BA 108 cloud has a significantly higher line strength. Thus, if there are GMCs with

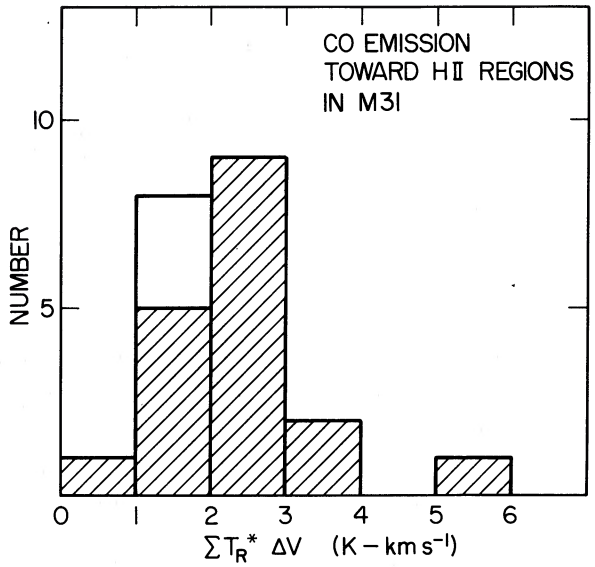

FIG. 3.—Histogram of the velocity-integrated CO emission toward the H II regions in M31. The unshaded portion indicates the three probable detections. The few objects detected below 1 K km s^{-1} indicate that this value is probably the most reasonable estimate of the sensitivity limit. No individual H II regions show emission in excess of 3.2 K km s^{-1}. The point at 5.7 K km s^{-1} is a region where 6 H II regions are clustered in the beam.

$\sum T_R^* \Delta V$ greater than 3 K km s^{-1} in M31, they must be very rare. Because most of the emission may be from small clouds not associated with the GMCs (see previous section), the limiting line strength for GMCs in M31 is likely to be considerably smaller. In any event, the cutoff seen in Figure 3 indicates a cutoff in the properties of GMCs in M31.

The most sensitive factor in the observed line strength is almost surely beam filling; the mean integrated line strength for several GMCs in the solar neighborhood averaged over the entire cloud shows little variation. Similarly, typical antenna temperatures of clouds identified in CO surveys of the inner Galaxy rarely exceed ~ 6 K, indicating that the mean peak antenna temperature of GMCs is not a highly variable quantity. Therefore, the quantity most responsible for the observed antenna temperature of extragalactic GMCs if they are like their Milky Way counterparts is size. The cutoff seen in Figure 3 implies that the GMCs in M31 are limited in size as are those in the Milky Way (Blitz 1978, 1980).

Stark and Blitz (1978) argued that the sizes and masses of local GMCs are consistent with the idea that they are limited by the tides of the Galaxy. The same appears to be true of the GMCs in M31. Since the rotation curve of M31 is approximately flat, with a circular velocity of ~ 250 km s^{-1}, the tidal acceleration per unit length T is similar to that for the Milky Way in the region in which most of the clouds in Table 1 are detected. Figure 2 of Stark and Blitz shows that T varies by less than a factor of 2 between 5 and 10 kpc from the center; extrapolation to $R = 12$ kpc, the most distant detection in M31, produces an additional change of less than 50%. Thus the detected GMCs in M31 are subject to an approximately constant tidal acceleration, very similar to that in the Milky Way. Since the sizes and masses of the GMCs in M31 do not appear to be larger than their Galactic counterparts, the sizes of GMCs in M31 also appear to be tidally limited.

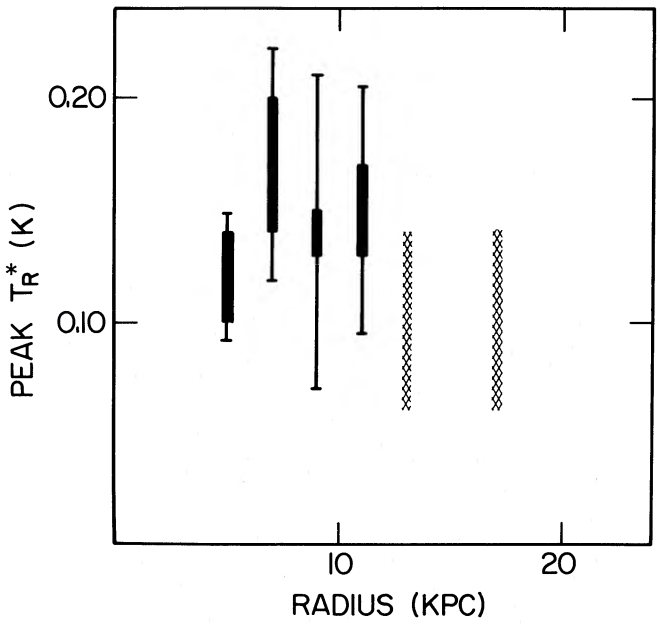

FIG. 4.—A plot of peak antenna temperature T_R^* as a function of radius plotted in 2 kpc bins. The middle of the solid bar is the mean value, and the extent of the bar is the 1 σ uncertainty of the mean. The extent of the narrow bar is the dispersion of the value of T_R^* within the radial bin. The lightly shaded bars are the probable detections BA 484 and BA 248. The mean values are weighted by the uncertainty of the observations, and the probable detections get half-weight.

v) *Radial Trends*

To see whether there are any trends in the CO emission with radius, the quantities T_R^*, ΔV, and $T_R^* \Delta V$ are averaged in 2 kpc bins plotted in Figures 4–6. The solid bar indicates the 1 σ uncertainty of the weighted mean value of the quantity plotted; the thin line extending from the bar is the dispersion of the quantity in each bin. The lightly shaded bars are for the uncertain detections BA 484 and BA 248. The quantities T_R^* and ΔV show no trend with radius. The innermost point in Figure 5 shows a marginal increase, consistent with the larger differential rotation expected for the clouds nearest the center of M31. The near-constancy of ΔV beyond this point is consistent with a constant velocity dispersion as a function of distance in the small-cloud component.

The plot of $\sum T_R^* \Delta V$ shown in Figure 6, on the other hand, shows an apparent decrease with radius. That the decrease beyond $R = 12$ kpc is real is illustrated by Figures 2 and 3. Figure 2 shows that the percentage of detections drops markedly beyond $R = 12$ kpc. Figure 3 shows that the sensitivity limit of the observations is ~ 1 K km s^{-1}. Thus the mean value for $\sum T_R^* \Delta V$ beyond $R = 12$ kpc *when the nondetections are included* is less than ~ 0.5 K km s^{-1}. Since the detection percentage from $R = 4$–10 kpc is greater than 50%, the mean $\sum T_R^* \Delta V$ in this range is greater than 1 K km s^{-1} when account is taken of the nondetections. It therefore appears that the mean integrated antenna temperature within the beam is a decreasing function of galactic radius. If, as discussed in § IV*a*(iii), most of the emission is from small clouds, and the small clouds are similar to their Milky Way counterparts, then the decrease shown in Figure 6 is unrelated to the radial decrease in the disk light (and presumably disk mass). This is because most of the star formation in the Milky Way takes place in giant molecular clouds (e.g., Blitz 1978) and there appears to be relatively little star formation in the small molecular clouds (Magnani, Blitz, and Mundy 1985).

The radial decrease in $\sum T_A^* \Delta V$ may, however, be related to the abundance gradient found in M31 (Blair, Kirshner, and Chevalier 1982). These authors find that the O/H ratio drops by about a factor of 4 from $R = 5$ to $R = 20$ kpc in M31. This is similar to the decrease shown in Figure 6, although the uncertainties are large. If the gradient in $\sum T_A^* \Delta V$ is due to a lower oxygen (and perhaps also carbon) abundance, the mass of H_2 within the beam could be relatively constant as a function of radius. In any event, the gradient of H_2 surface density would be less steep than that of the CO. A similar effect has

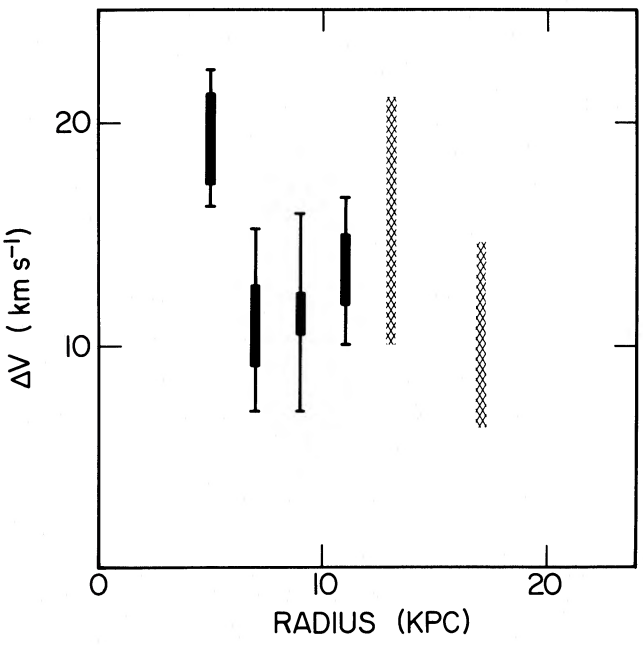

FIG. 5

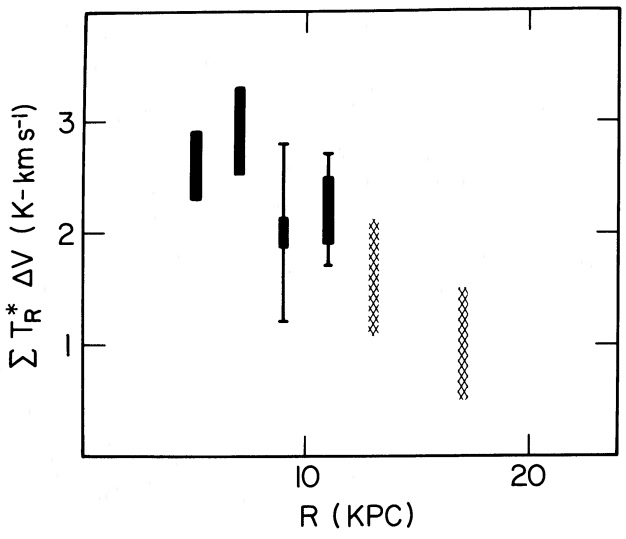

FIG. 6

FIG. 5.—Same as Fig. 4, but for the line width ΔV. The minimum uncertainty for the line width determination is taken at 2.6 km s^{-1}, regardless of the fitted value given in Table 1.

FIG. 6.—Same as Fig. 4, for $\sum T_R^* \Delta V$. There is an apparent decrease of this quantity with radius.

already been pointed out for M101 (Blitz 1985). Alternatively, the radial gradient of $\sum T_A^* \Delta V$ could be due to a decrease in the filling fraction of the molecular clouds in the beam.

b) M33

Of the six clouds observed in M33, there are two detections, the spectra of which are shown in Figure 4, two possible detections, and two nondetections. For both the detections and the possible detections, the peak antenna temperatures are comparable to the values observed in M31, but the lines are narrower. The velocity-integrated temperatures are therefore considerably lower in M33.

Of the six H II regions observed, the strongest CO line has $\sum T_R^* \Delta V = 1.3$ K km s^{-1}. This value is only twice that expected from local GMCs at the distance of M33. Even if there were no emission from small clouds in the beam, the observed upper limit implies that the limiting mass for GMCs in M33 is not much greater than that found locally in the Milky Way. The relatively small number of H II regions observed in M33, however, makes this conclusion somewhat tentative.

It is more significant perhaps that the two detections are from the extraordinary H II regions NGC 604 and NGC 595. The radio continuum fluxes from these objects are generated by the equivalent of 113 and 37 O6 stars, respectively (Israel and van der Kruit 1974). The molecular emission from these objects is not, however, extraordinary, and is within a factor of 2 of what would be expected from local GMCs at the distance of M33. Thus, if the H_2 masses of these complexes are proportional to their CO luminosities, the virulent star formation is not associated with extraordinarily massive GMCs.

It should be pointed out, however, that Israel and van der Kruit (1974) derive ionized masses of 2.2×10^6 and 4.9×10^5 $M_\odot$ for NGC 604 and NGC 595, respectively, compared with an estimated upper limit of $\sim(3\text{–}4) \times 10^5$ $M_\odot$ of H_2. Thus, if the radio continuum emission comes primarily from ionized *molecular* gas, the parent molecular clouds may once have been quite massive. Furthermore, Dufour, Schiffer, and Shields (1985) have measured the abundances of carbon and oxygen in NGC 604 and find them to be underabundant by factors of 15 and 2.5, respectively, relative to abundances in the Orion Nebula. The low CO luminosity of NGC 604 may simply be a reflection of its very low metallicity.

As for M31, one can estimate what fraction of the CO emission is from small molecular clouds like those found in the solar neighborhood. The inclination angle of M33 is $\sim 45°$; thus, following the discussion in § IV*a*(ii), the observed peak antenna temperature from small clouds would be 0.04 K. The minimum line width would be about 13 km s^{-1}, but the broadening due to differential rotation would be smaller than that for M31. Thus the observed line width would be ~ 15 km s^{-1}, implying $\sum T_A^* \Delta V = 0.6$ K km s^{-1} for a population of small clouds like those found locally.

The present observations are not sufficiently sensitive to detect lines of this strength unambiguously. However, if this contribution is subtracted from the observed lines, the resulting $\sum T_A^* \Delta V$ is remarkably close to what would be observed for local GMCs at the distance of M33. The emission from the GMCs and that from the small clouds are expected to have different strengths ($\langle T_A^* \rangle = 0.14$ and 0.04 K, respectively) and different line widths ($\Delta V = 5$–8 and 15 km s^{-1}, respectively). If the observed line comes from a combination of these two populations, the observed line width should be intermediate between these two values when the emission is fitted by a single Gaussian as in the present observations. The mean of the two detections is 10.5 km s^{-1}, a value consistent with this hypothesis.

V. SUMMARY AND CONCLUSIONS

CO emission has been detected toward a number of H II regions in M31 and M33. Most of the CO emission in the direction of the Baade and Arp H II regions in M31 appears to originate in small molecular clouds, possibly similar to those recently discovered in the vicinity of the Sun. The emission from giant molecular clouds like those within ~ 2 kpc of the Sun would account for only $\sim \frac{1}{4}$ of the CO emission observed with the 66″ beam at NRAO. With smaller beams, the relative contribution of the GMCs to the CO emission should increase, and the CO lines should become narrower. Specific observational predictions are made as to what would be observed with very high resolution ($\leq 30''$). There is no evidence that the GMCs in M31 are different from those in the Milky Way.

The peak line strength and line width show no significant radial dependence in M31. However, the integrated line strength, $\sum T_R^* \Delta V$, does show a significant decrease with galactic radius. The decrease is most probably due either to a metallicity gradient or to a decrease in the surface filling fraction of the small clouds in the telescope beam. No individual GMC in either M31 or M33 is observed with $\sum T_R^* \Delta V$ in excess of 3.2 K km s^{-1}, indicating that the clouds have a natural size limit which may be tidally determined.

The contribution from small clouds is less in M33 than in M31 because the former is less inclined to the line of sight. The CO emission from the two detected H II regions NGC 604 and NGC 595 is comparable to that which would be observed from galactic GMCs mixed with a population of small clouds at the distance of M33. These spectacular H II regions do not, however, have extraordinary molecular emission associated with them. If the mass of ionized gas is primarily the result of ionization of the *molecular* gas, the molecular clouds may once have been very massive. Alternatively, the low metallicity in NGC 604 may mask a relatively high associated H_2 mass.

This work was begun when the author was associated with the Radio Astronomy Laboratory of the University of California. The work was partially supported by grants AST 78-21037 and AST 83-15276 from the National Science Foundation. I wish to thank Adair Lane for assistance with some of the observing and data reduction, and Tony Stark for his isovelocity contour plot. I have also received thoughtful comments on the manuscript from the referee, Frank Israel, as well as from Françoise Combes, Tony Stark, and Fran Verter.

REFERENCES

Baade, W., and Arp, H. 1964, *Ap. J.*, **139**, 1027.
Blair, W. P., Kirshner, R. P., and Chevalier, R. A. 1982, *Ap. J.*, **254**, 50.
Blitz, L. 1978, Ph.D. thesis, Columbia University.
———. 1980, in *Giant Molecular Clouds in the Galaxy*, ed. P. M. Solomon and M. G. Edmunds (Oxford: Pergamon), p. 1.
Blitz, L. 1985, comment following paper by J. Young in *IAU Symposium 106, The Milky Way Galaxy*, ed. H. van Woerden, W. B. Burton, and R. J. Allen (Dordrecht: Reidel), p. 190.
Blitz, L., Fich, M., and Stark, A. A. 1982, *Ap. J. Suppl.*, **49**, 183.
Blitz, L., Magnani, L., and Mundy, L. 1984, *Ap. J. (Letters)*, **282**, L9.

Blitz, L., and Thaddeus, P. 1980, *Ap. J.*, **241**, 676.
Blitz, L., and Mathieu, R. D. 1985, in preparation.
Boulanger, F., Bystedt, J., Casoli, F., and Combes, F. 1984, *Astr. Ap.*, **140**, L5.
Boulanger, F., Stark, A. A., and Combes, F. 1981, *Astr. Ap.*, **93**, L1.
Brinks, E. 1984, Ph.D. thesis, University of Leiden.
Dame, T. 1983, Ph.D. thesis, Columbia University.
Dufour, R. J., Schiffer, F. H., and Shields, G. A. 1985, preprint.
Ichikawa, T., Nakano, M., Tanaka, Y. D., Saito, M., Nakai, N., Sofue, Y., and Kaifu, N. 1985, preprint.
Israel, F. P., and van der Kruit, P. C. 1974, *Astr. Ap.*, **32**, 363.
Kutner, M. L., and Mead, K. 1981, *Ap. J.* (*Letters*), **249**, L15.
Kutner, M. L., Tucker, K. D., Chin, G., and Thaddeus, P. 1977, *Ap. J.*, **215**, 521.
Kutner, M. L., and Ulich, B. L. 1981, *Ap. J.*, **250**, 341.
Lada, C. J., Elmegreen, B. G., Cong, H. I., and Thaddeus, P. 1978, *Ap. J.* (*Letters*), **226**, L39.
Linke, R. A. 1982, in *Extragalactic Molecules*, ed. L. Blitz and M. L. Kutner (Green Bank: NRAO), p. 87.
Magnani, L., Blitz, L., and Mundy, L. 1985, *Ap. J.*, in press.
Rogstad, D. H., Wright, M. C. H., and Lockhart, I. A. 1976, *Ap. J.*, **204**, 703.
Rubin, V. C., and D'Odorico, S. 1969, *Astr. Ap.*, **2**, 484.
Sanders, D. B., Solomon, P. M., and Scoville, N. Z. 1984, *Ap. J.*, **276**, 182.
Stark, A. A. 1983, in *Kinematics, Dynamics and Structure of the Milky Way*, ed. W. L. H. Shuter (Dordrecht: Reidel), p. 127.
Stark, A. A. 1985, in *IAU Symposium 106, The Milky Way Galaxy*, ed. H. van Woerden, W. B. Burton, and R. J. Allen (Dordrecht: Reidel), p. 445.
Stark, A. A., and Blitz, L. 1978, *Ap. J.* (*Letters*), **225**, L15.
Wouterloot, J. G. A. 1981, Ph.D. thesis, Leiden University.
———. 1984*a*, *Astr. Ap.*, **134**, 244.
———. 1984*b*, *Astr. Ap.*, **135**, 32.

LEO BLITZ: Astronomy Program, University of Maryland, College Park, MD 20742